A Case Study of Two-Dimensional Stratified Turbulence

ULF HÖGSTRÖM, ANN-SOFI SMEDMAN, AND HANS BERGSTRÖM

Department of Earth Sciences, Meteorology, University of Uppsala, Uppsala, Sweden

(Manuscript received 15 April 1997, in final form 18 April 1998)

ABSTRACT

Data from a period with intensive measurements in the lowest 1000 m of a marine atmosphere over the Baltic Sea with strongly stable stratification and a turbulent boundary layer less than 50 m deep have been analyzed with respect to the mesoscale flow regime.

Analysis of the wind data shows that horizontal wind fluctuations take place in vertically decoupled layers of the order of a few hundred meters deep. In spite of sometimes large shear, turbulence levels are shown to be very low, implying a ''dissipation travel distance'' of the order 1000 km.

Airborne measurements have been used to produce wavenumber spectra of the zonal and meridional components of the wind and the temperature over the spectral range $10^{-4} \leq \kappa \leq 1$ radians m^{-1} and frequency spectra for the vertical wind component. Extended series of continuous wind measurements on a tower were used to derive frequency spectra of the wind, which were Taylor-transformed to wavenumber spectra, showing good agreement with the spectra derived from the airborne measurements.

The horizontal wavenumber spectra show no significant height variation for the 30–500-m layer studied. For the approximate wavenumber range $10^{-5} \leq \kappa \leq 10^{-3}$ radians m^{-1}, these spectra fall off as $\kappa^{-5/3}$, with a spectral level only about a factor of 2 lower than the corresponding Global Atmospheric Sampling Program spectra from the upper troposphere and the lower stratosphere. Vertical velocity spectra are very close in shape and spectral amplitude to corresponding spectra derived from Doppler radar measurements at several places around the world during ''quiet-time conditions.'' However, an important difference of the present spectra is that they show no sign of scaling with the local Brunt–Väisälä frequency. The temperature spectra are closely similar in shape to the horizontal velocity spectra, and their amplitude scale with the square of the local Brunt–Väisälä frequency. Detailed analysis of the spectra for this wavenumber range suggests that the spectra of horizontal motion reflect quasi-two-dimensional stratified turbulence, but that the vertical velocity spectra reflect wave activity.

In the wavenumber range $10^{-3} \leq \kappa \leq 10^{-2}$ radians m^{-1} the horizontal wind spectra fall off approximately as $\kappa^{-9/4}$, which suggests that internal waves may make up this spectral region, an assertion that is also supported by application of a polarization relation valid for waves. Temperature–vertical velocity cross spectra show no signs of linear, monochromatic waves. Instead it is possible that the waves in this region are breaking, a process that has previously been suggested as a possible source for the quasi-two-dimensional turbulence.

1. Introduction

The atmospheric spectral range representing wavelengths approximately from a few kilometers and up to 500 or 1000 km is sandwiched between the baroclinic range at the larger-scale end and three-dimensional turbulence at the small-scale end (if present at all). The motions in this range are known to be nearly horizontal. The statistical properties of this range have been thoroughly mapped by measurements obtained from over 6900 commercial aircraft flights made during the Global Atmospheric Sampling Program (GASP) and presented in papers by Nastrom and Gage (1985) and Gage and Nastrom (1986a,b). It is clear from these measurements (Fig. 1) that wind as well as temperature spectra adhere to predictions from the general theory for two-dimensional turbulence presented by Kraichnan (1967) in having a $\kappa^{-5/3}$ range for wavenumbers, κ, between roughly 10^{-3} and 10^{-5} radians m^{-1}, and a κ^{-3} range for the wavenumber decade below 10^{-5} radians m^{-1}; see section 6 for a discussion.

Nevertheless, the question of the origin and true nature of the motions seen in these spectra is not entirely settled. Thus VanZandt (1982) and others argue that the observed spectra are due to gravity waves. Gage and Nastrom (1986a) in their theoretical interpretation of the GASP measurements and some complementary vertical velocity spectra conclude that the horizontal motions are indeed due to two-dimensional turbulence, whereas in their opinion, the vertical velocities are likely to reflect internal wave activity.

The theory for stratified turbulence was expounded by Lilly (1983). He introduced the idea that the source

Corresponding author address: Dr. Ulf Högström, Department of Earth Sciences, University of Uppsala, Geocentrum, Villavägen 16, S-75236 Uppsala, Sweden.
E-mail: ulf@big.met.uuse

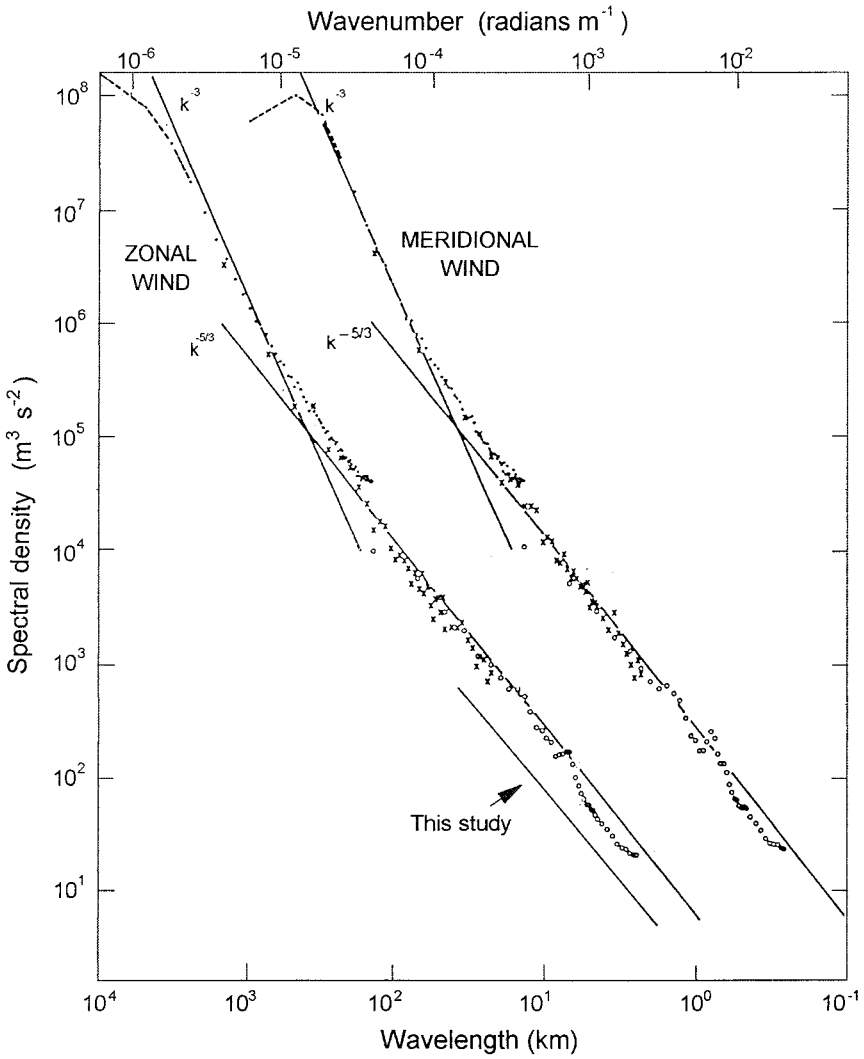

FIG. 1. Wavenumber spectra of zonal and meridional velocity from the GASP measurements. The straight lines indicate slopes of -3 and $-5/3$. Also included is a curve derived from the present study (cf. Fig. 10). The meridional spectra are shifted one decade to the right (after Gage and Nastrom 1986a).

for the stratified mesoscale turbulence is strong convection. Thus originally three-dimensional turbulence is being squeezed to become very nearly two-dimensional. During this process energy is transferred through the spectrum from smaller to larger scales. Thus a reverse cascade process is predicted and a spectral $\kappa^{-5/3}$ range as well. At large enough scales (order of thousands of kilometers) energy is being produced by baroclinicity and eddy enstrtophy (mean squared vorticity) is being transferred to smaller scales, a process that was predicted by Kraichnan (1967) and Batchelor (1969) to result in a κ^{-3} spectral range. The situation is schematically represented in Fig. 2. Gage and Nastrom (1986a) argue that the small-scale energy source (at wavelengths of the order of kilometers) is more likely to be breaking internal waves than convection.

Some of the results from Lilly's (1983) theoretical work will be used for interpretation of the new experimental results presented in the present paper. In particular, it will be possible to test Lilly's prediction that his solution of the equations of motion for stratified turbulence would correspond to quasi-two-dimensional motions in vertically decorrelated layers. The measurements are also amenable to an analysis of the effect of friction, which was of some concern for Lilly (1983), who argued that decorrelation would lead to large shear and possibly to rapid dissipation.

The experimental data consist of measurements in the lowest 1000 m of a strongly stable marine airflow from what was originally designed to be a boundary layer experiment. It turned out, however, that stability was so strong that the vertical extension of the actual boundary

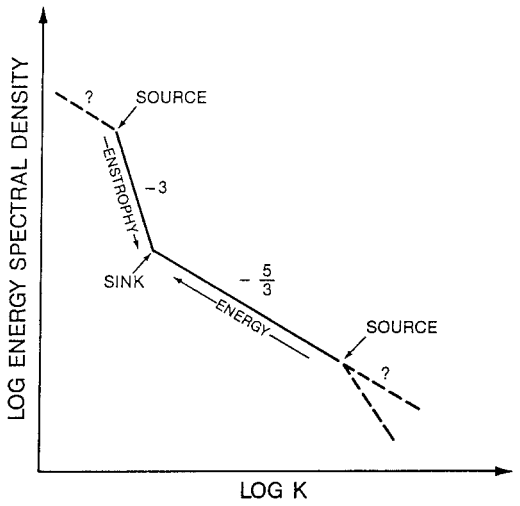

FIG. 2. Schematic representation of spectral ranges in quasi two-dimensional turbulence (after Larsen et al. 1982).

layer was only of the order of a few tens of meters and that turbulence in that layer was mostly continuous but of very low intensity. Thus the term ''quasi-frictional decoupling'' was coined to characterize this situation. The turbulence regime of this rather special boundary layer is reported elsewhere (Smedman et al. 1997).

The measurements, which include airborne measurements, radiosoundings, and tower measurements, were taken over the Baltic Sea during the period 29 May–15 June 1995 and are described in detail in section 2.

The synoptic situation during the measuring campaign was rather persistent, with a high pressure ridge extending from Russia toward the northeast and a weak low pressure area to the southwest. Thus, the general flow over the Baltic Sea was from the southeast or from the south, with a typical speed of 7–8 m s^{-1} at the top of the boundary layer. The friction velocity was only 0.08 m s^{-1} on the average; compare Smedman et al. (1997). Most of the time there was little cloudiness, but on two occasions weak fronts passed the area. The surface temperature of the Baltic Sea was below 10°C at the onset of the measuring campaign, rising gradually to about 13°C at the end. Midday temperatures over the upwind land areas of the Baltic states and Poland were typically above 20°C, being around 28°C during the period 29 May–1 June, which is the core period for the study reported in this paper.

The presentation of the site and the measurements in section 2 is followed in section 3 by a general discussion of the characteristic features of the flow regime. In section 4 an analysis of the wind data is carried out. In section 5 a similar analysis of the temperature field is made. A theoretical interpretation of the flow regime is attempted in section 6, followed by conclusions in section 7.

2. Site and measurements

The island Östergarnsholm is situated about 4 km east of the big island of Gotland; see Fig. 3. Östergarnsholm is a low island with no trees. A 30-m tower has been erected at the southernmost tip of the island. The base of the tower is situated at just about 1 m above mean sea level. The approximate sector 60°–220° is characterized by more than 150 km undisturbed upwind over water fetch.

During the 1995 campaign the 30-m tower was instrumented with slow response (''profile'') sensors of in-house design for temperature and for wind speed and direction at the following heights above the tower base: 7, 11.5, 14, 20, and 28 m. Turbulent fluctuations were recorded with an MIUU (Institute of Meteorology, Uni-

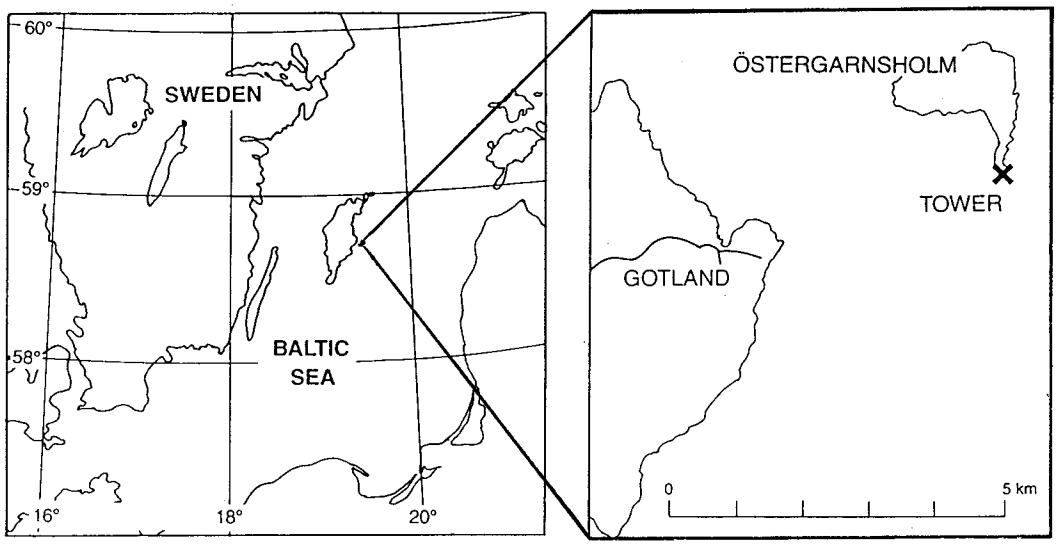

FIG. 3. Map of the Baltic Sea with a close-up of the site Östergarnsholm.

versity of Uppsala) turbulence instrument at 9 m (for details see Smedman et al. 1997; Högström 1982, 1988). Profile data were recorded at 1 Hz and turbulence data at 20 Hz.

Radiosoundings with Vaisala RS80 sondes were made from Östergarnsholm on 16 occasions during the most intensively studied time period, 29 May–1 June 1995. During this period additional pilot balloon measurements were made on 12 occasions. During most of these events three balloons were released in succession during typically 20–30 min. The balloons were followed to 1000–2500-m height. Also, most radiosoundings were accompanied by two additional pilot balloons. During the same time period airborne measurements were performed on eight occasions. An additional 15 radiosoundings, 9 pilot balloon measurements, and 4 airborne missions were conducted during the time period 6–15 June 1995. Some of these data are also used in the analysis (primarily the airborne measurements).

Airborne measurements were performed with an instrumented Sabreliner 40A twin jet aircraft. The instrumentation and evaluation procedure is described in detail in Tjernström and Friehe (1991). Wind measurements were performed using the so-called radome gust probe technique (Brown et al. 1983), where the local wind vector relative to the aircraft fuselage is inferred from measurements of the pressure distribution over the radome of the aircraft in combination with ambient air temperature and static pressure. The aircraft horizontal velocity vector, vertical acceleration, and attitude angles relative to the earth are obtained from an inertial navigation system (INS), a Litton LTN-72. Air temperature is measured with a standard Rosemount 102EAL total temperature probe.

The accuracy of the mean wind speed degrades with time due to long-term errors induced by the INS but is estimated to be better than ± 0.5 m s^{-1} for typical flight times with the present aircraft. The relative error, which is important for calculation of turbulent quantities, is less than ± 0.1 m s^{-1}.

All flights were flown at a true airspeed of 100 m s^{-1}. Each aircraft mission started and ended with a ''slant profile,'' flown in the height interval 100–2000 m with a constant vertical aircraft velocity of 4–5 m s^{-1}. These profiles were flown over the Baltic Sea in an area some 40–50 km northeast of Östergarnsholm. In the 70–85-min time period between the profiles straight flight paths at constant altitude were flown along a line extending from Östergarnsholm and 50 km either to the northeast, east, or southeast. During each individual mission exactly the same horizontal track was flown but at a number of altitudes, typically 30, 60, 90, 150, 180, and 210 m, sometimes supplemented with flights around 400 or 500 m. Most heights were flown in both directions (and sometimes a third time in the first direction). All flights, except that at 30 m, covered the entire 50-km track. For security reasons, the 30-m flights were limited to the distance interval between 20 and 40 km from Östergarnsholm.

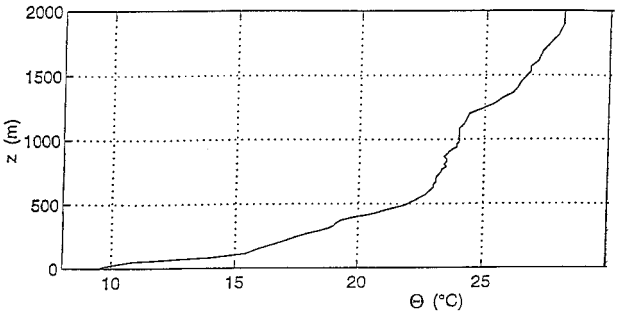

FIG. 4. Vertical profile of potential temperature measured on 29 May 1995 at 1053 LST.

3. General characteristics of the situation 29 May–15 June 1995

The profile of potential temperature shown in Fig. 4 is typical for most of the time during the experiment. Only in relation to the passage of a few weak fronts were other temperature profiles temporarily observed. Characteristic of the profile in Fig. 4 is the very stable stratification in the lowest few hundred meters above the sea surface. Thus there is no indication of a transition to a mixed layer profile in spite of the more than 150-km travel distance over water.

The existence of this very deep stable layer close to the sea surface shown in Fig. 4 calls for an explanation. Simulations with a numerical boundary layer model clearly reveal that the observed thickening of the stable layer is a blocking effect of the big island of Gotland, which is situated a few kilometers downstream of Östergarnsholm for winds from an easterly direction (Fig. 3); see the appendix for details.

The wind profile in the lowest 1000 m is very irregular and changes shape from sounding to sounding. Nevertheless, the variations between individual balloons composing one profile is almost always small. Figure 5 is a typical example of such measurements, including also a graph of the corresponding wind direction profile. The characteristics of the wind variations are analyzed in section 4.

Wind speed and temperature measured at 4- and 5-m heights on the 30-m tower exhibit very characteristic traces, as illustrated for one day, 30 May, in Figs. 6 and 7. Variations on all timescales, from minutes to several hours, are seen to be highly coherent at every level, in particular for temperature. Fluctuations in both wind speed and temperature are large and, sometimes, rapid. Thus, temperature at the highest measuring level, 30 m, varied from below 12° to close to 18°C during this day (Fig. 6). These variations are not likely to be related to sea surface temperature variations. At least there were no such variations observed at a nearby wave buoy site

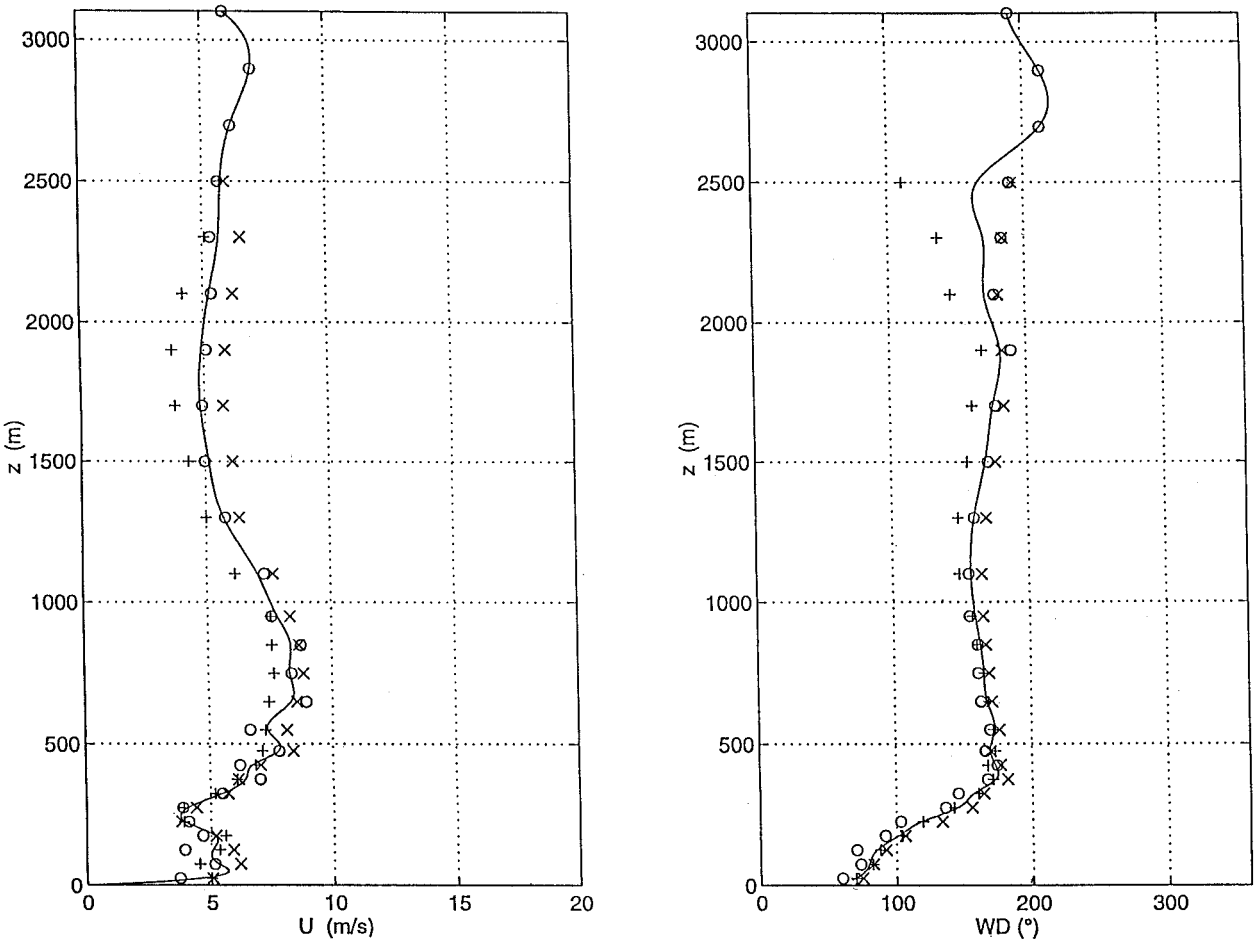

FIG. 5. Vertical profiles of wind speed and direction measured on 30 May 1995 at 1312 LST. The different symbols refer to different balloons released in succession during a period of about 20 min.

(the buoy was moored roughly 5 km south-southeast of the tower), where sea surface temperature was found to increase gradually from 9.5° to 10.7°C during the day. As shown in Fig. 7, wind speed at 30 m varied from from 2 to 8 m s^{-1} during the same day. Wind direction was measured at all four profile levels as well. Plots (not shown here) similar to that of temperature and wind speed show that wind direction exhibited large variations during the course of a typical day, but with hardly any variation with height at any time in the 30-m layer covered by the tower.

4. Analysis of the wind data

a. The horizontal wind field

The analysis of this subsection is confined to data from the first part of the measuring period, that is, 29 May–1 June 1995. During this period 28 pilot balloon wind profiles, most of which include three balloons, are available. Table 1 gives the wind speed mean values and standard deviations for 15 m (from the tower) and from the levels 100, 200, 400, 600, 800, and 1000 m from pilot balloon measurements. The mean of the standard deviation for all levels is 1.84 m s^{-1}. This should be compared with the mean standard deviation among the individual balloons relative to the computed mean wind profile for each measurement case, 0.75 m s^{-1}. This means that the variance during a balloon sounding, which takes between 20 and 30 min, is only about 17% of the total variance. Thus, more than 80% of the total wind variance is due to fluctuations with timescales longer than that.

Time plots of measured wind speed at all heights (not shown here) reveal that wind speed variations already at 100-m height is only partially related to those recorded on the tower and that for higher levels there is very little correlation with the ''tower wind.'' Plotted in Fig. 8 are computed autocorrelations of wind speed, relative to each measuring height in turn. From all plots it is clear that complete decorrelation (correlation coefficient, $r = 0$) occurs over the measuring range for all heights.

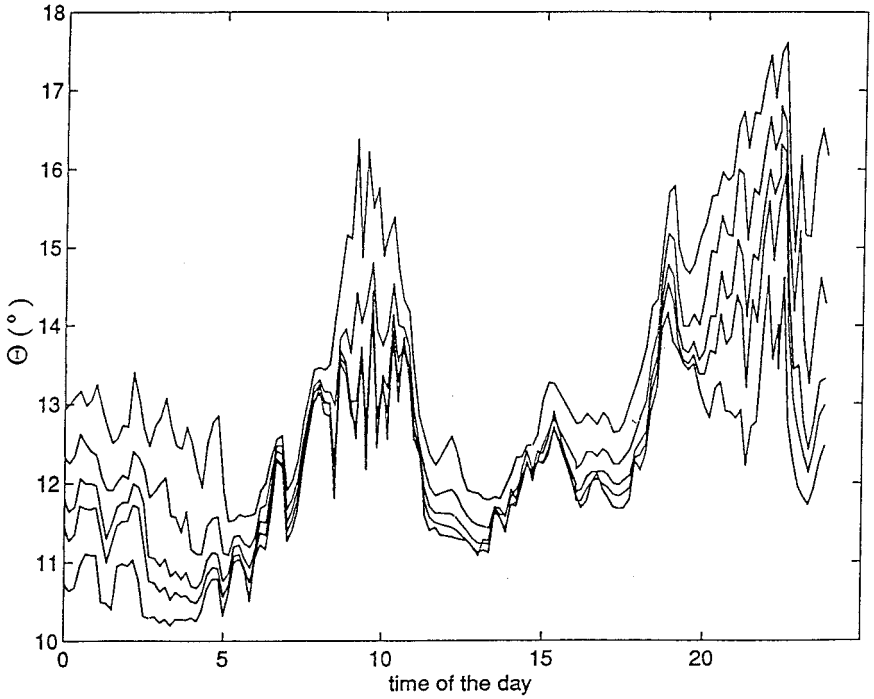

FIG. 6. Time series of potential temperature measured at five levels on the tower (6.9, 11.9, 14.3, 20.2, and 28.8 m above ground) on 30 May 1995.

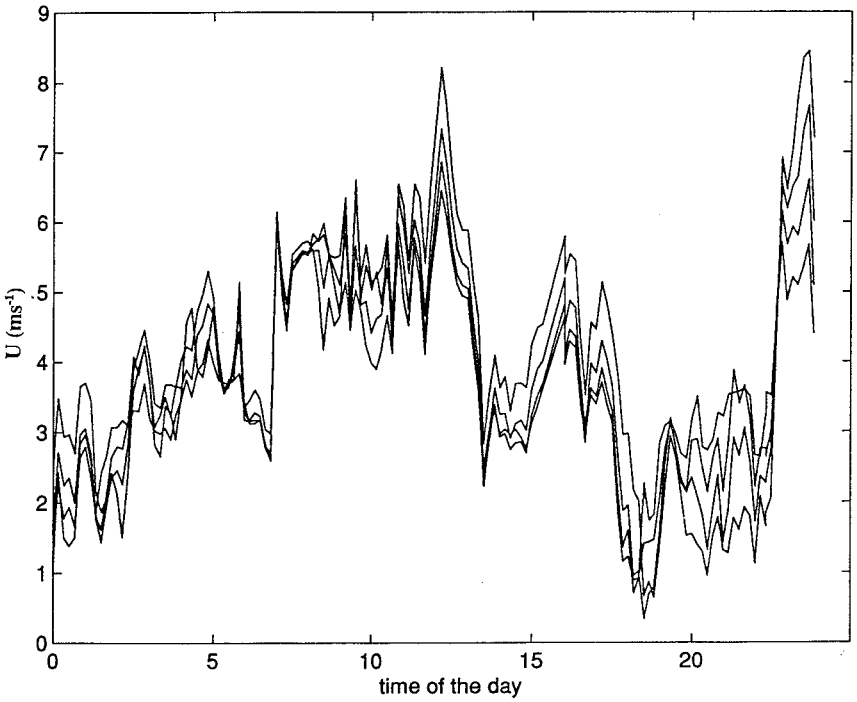

FIG. 7. Time series of wind speed measured at four levels (one anemometer was out of order) on the tower (6.9, 14.3, 20.2, and 28.8 m above ground) on 30 May 1995.

TABLE 1. Mean and standard deviation of wind speed (m s^{-1}) at selected heights in the lowest 1000 m derived from the 28 balloon measurements during the time period 29 May–1 June 1995. The 15-m data are taken from the tower measurements.

	15 m	100 m	200 m	400 m	600 m	800 m	1000 m
Mean	3.59	4.71	4.93	5.03	6.37	7.24	7.76
Std dev	1.21	2.21	1.68	2.06	1.67	1.74	1.66

Defining arbitrarily the vertical distance from the reference height to the height where the correlation, $r = 0.5$ as a ''correlation half-width,'' h_c, the following result is obtained: $z = 15$ m, $h_c = 50$ m; $z = 100$ m, $h_c = 100$ m; $z = 200$ m, $h_c = 150$ m; $z = 400$ m, $h_c = 250$ m; $z = 600$ m, $h_c = 350$ m; $z = 800$ m, $h_c \approx 350$ m; $z = 1000$ m, $h_c \approx 350$ m (estimate based on lower half-width only). Thus the horizontal velocity variations observed during this time period become vertically decorrelated for height separations of the order of a few hundred meters.

A similar analysis was conducted with respect to the wind direction variations, which were obtained from the tower at 15 m and from the pilot balloon measurements at the same six heights as wind speed (cf. above). Standard deviation of the wind direction fluctuations were as high as 63° for 15 m and 41° for 100 m, decreasing gradually to 23° for 1000 m. The result of an autocorrelation analysis (not shown here) is similar to that shown for wind speed in Fig. 8, with about the same correlation half-width values as for wind speed. There is, however, one difference. Correlation at large distance does not go down to zero as does the corresponding wind speed autocorrelation. Instead, the direction autocorrelation levels out at about $r = 0.3$, implying that about 10% of the variance is common to the entire 1000-m layer. This is probably the result of a minor synoptic variation. Nevertheless, the dominating part of the wind direction variability (about 90%) is due to variations in vertically decorrelated layers just as was found to be the case for wind speed.

b. Turbulent friction

Two independent analyses were done: (i) the local gradient Richardson number was determined for every

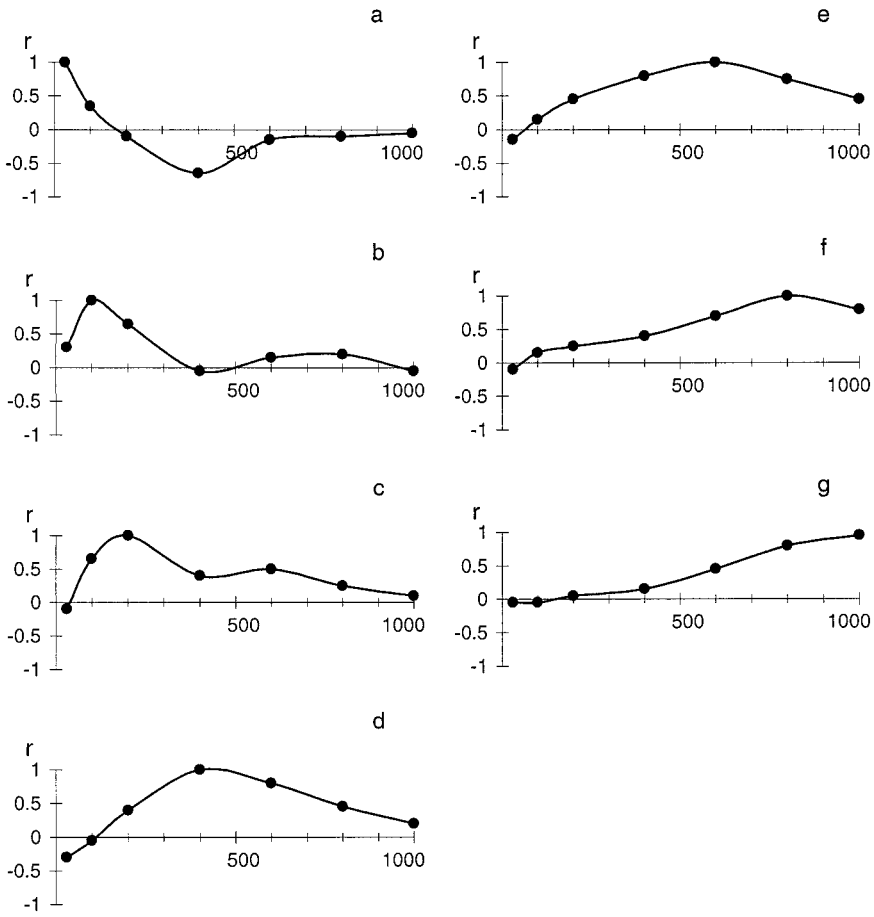

FIG. 8. Autocorrelation coefficient for the horizontal wind speed measured at seven levels from 15 to 1000 m. (a) How the correlation varies with height relative to the measurements at 15 m; (b)–(g) The correlation plotted relative to the measurements at 100, 200, 400, 600, 800, and 1000 m, respectively.

TABLE 2. Gradient Richardson numbers derived from radio soundings from the time period 29 May–1 June 1995 (times are LST). Wind and potential temperature gradients have been obtained from tangent drawn to the respective curves at the selected heights. Values below the critical Richardson number, 0.25, are italic and values between 0.25 and 1.0 are bold.

Time		100 m	200 m	400 m	600 m	800 m	1000 m
29 May	1050	135	14	4.6	6.1	*0.17*	7.7
	1445	40	32	300	2.2	22	2.8
30 May	1500	3.2	100	12	34	1.8	13
	2200	1.5	**0.7**	2.1	2.8	1.9	
31 May	0100	4.1	**0.5**	15	350	12	360
	0514	1.2	21	4.8	19	20	
	0850	2.3	*0.06*	3.7	1.7	220	**0.9**
	1650	4.1	**0.6**	2.1	**0.5**	6.6	**0.6**
	2104	2.2	13	1.2	1.2	1.2	*0.23*
1 Jun	0109	5.1	1.0	**0.39**	17	18	1.3
	0503	>100	**0.43**	14	3.8	>100	35
	0800	155	16	9	39	11	>100
	1209	5.3	**0.33**	1.3	2.5	90	4.5
	1432	**0.41**	2.2	19	13	12	1.2

radiosounding and for each of the 6 heights 100 m, . . . , 1000 m used in the above study of the horizontal wind variability; and (ii) the turbulent production term for each flight and flight level was determined.

Gradient Richardson number was calculated from radiosonde temperature profiles (like Fig. 4) and simultaneous wind profiles (cf. Fig. 5) by drawing tangents to the respective curves at the six heights and reading the corresponding gradient values from the graphs. The result of the calculations is shown in Table 2.

From this table it can be seen that Ri is less than its critical value, 0.25 in only 3 out of a total of 82 values. If the Ri range is extended to 1.0, thus including a possible hysteresis effect, 13 values are found to be lower than the limit for possibly occurring turbulence.

Turbulent production was derived in the following manner. For every flight and height, a mean value for $\overline{u'w'}$ was determined. Then the mean wind gradient $\partial U/\partial z$ was determined for the same heights from the pilot balloon soundings closest in time to the flights. Finally, the turbulent production term $-\overline{u'w'}\partial U/\partial z$ was calculated; see the first column of Table 3. Inspection of these figures reveals the occurrence of sporadic negative values, with all but one |value| $\leq 10^{-5}$ m^2 s^{-3}. Setting a ''noise-level threshold'' of $\pm 10^{-5}$ m^2 s^{-3}, implying that all values of a magnitude less than that should be considered as not significantly different from zero, gives the ''filtered'' values in the last column of the table. Thus, only 6 values out of 28 have production values that differ significantly from zero. The mean of all ''unfiltered'' values is 7×10^{-6} m^2 s^{-3}. The corresponding mean of the values in the column for filtered values is 8.7×10^{-6} m^2 s^{-3}, which, considering that the recorded production levels are probably close to the detection level, must be regarded as reasonably close to the unfiltered mean value.

Aircraft data from all but the last flight (wind from over the island) were used to deduce the buoyancy production (or destruction, as the case may be) term of the turbulence energy budget, $B = g/T_0\overline{w'\theta'}$. The overall mean for all flights (11) and heights (typically six to eight heights in each separate flight, ranging in height from 30 to 500 m) for B is -5.0×10^{-5} m^2 s^{-3}, with a standard deviation of 17.0×10^{-5} m^2 s^{-3} and standard error of the mean 5.0×10^{-5} m^2 s^{-3}. The average, taken

TABLE 3. Turbulent production, $-\overline{u'w'}\partial U/\partial z$ (m^2 s^{-3}), derived from simultaneous aircraft measurements (momentum flux) and pilot balloon soundings (wind gradient) from the time period 29 May–1 June 1995. The first row gives directly computed values. In the last row a noise filter has been applied, to the effect that all negative values and positive values $<10^{-5}$ m^2 s^{-3} have been replaced by zero. For each height, mean values of $u'w'$ has been derived over two or, sometimes, three 50-km flight legs along identical lines. Times indicate approximate midtime (LST) of flights.

Time		Height (m)	$-\overline{u'w'}\partial U/\partial z$	$-\overline{u'w'}\partial U/\partial z$ filtered
29 May	1430	155	-3.2×10^{-7}	0
		176	2.0×10^{-6}	0
		217	3.8×10^{-6}	0
30 May	1500	60	-2.2×10^{-5}	0
		90	0	0
		120	-3.1×10^{-6}	0
		275	6.8×10^{-6}	0
31 May	1000	60	5.3×10^{-6}	0
		90	7.6×10^{-6}	0
		120	1.2×10^{-6}	0
		180	2.9×10^{-5}	2.9×10^{-5}
31 May	1330	60	-6.5×10^{-7}	0
		90	1.8×10^{-5}	1.8×10^{-5}
		160	-6.3×10^{-6}	0
		360	3.0×10^{-5}	3.0×10^{-5}
31 May	1700	60	9.0×10^{-5}	9.0×10^{-5}
		90	1.1×10^{-6}	0
		160	5.8×10^{-5}	5.8×10^{-5}
		210	-5.8×10^{-6}	0
		460	-10^{-5}	0
1 Jun	1000	60	-2.6×10^{-6}	0
		90	1.9×10^{-5}	1.9×10^{-5}
		210	-9.3×10^{-6}	0
		460	-10^{-5}	0
1 Jun	1300	60	0	0
		90	-1.3×10^{-5}	0
		250	0	0
		460	6.0×10^{-6}	0

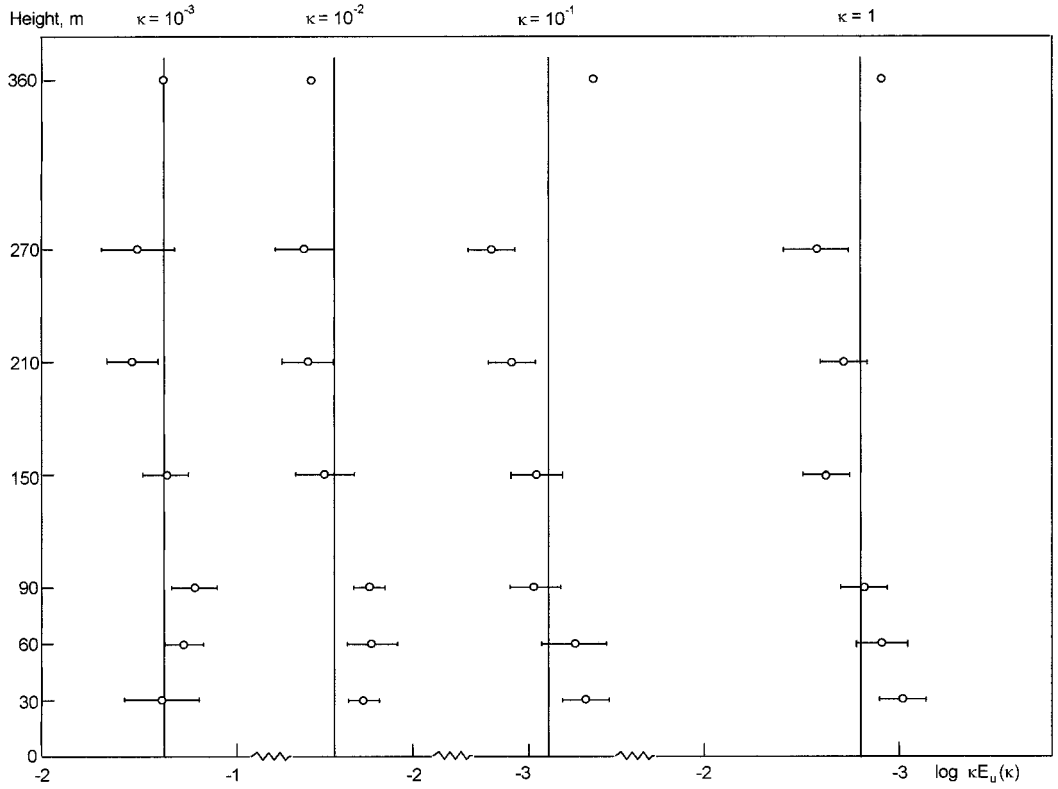

FIG. 9. Logarithm of the spectral amplitude of the zonal wind component derived from the 11 first flights plotted against measuring height for four selected wavenumber values, as indicated in the figure. Rings indicate mean values and horizontal bars the standard error of the mean for each height and wavenumber.

over all heights flown, is positive for four of the flights and negative for the remaining seven flights. The overall height variation (taken over all 11 flights) is such that the mean of B is positive for two heights, 30 and 200 m, and negative for 60, 90, 150, and 400 m. The observed fluxes are so small that they are likely to be mainly below the detection level. The apparent random height variation strongly supports this notion. The conclusion is that the buoyancy production term is not significantly different from zero.

An order of magnitude dissipation timescale can be obtained by assuming mean production = mean dissipation, $\varepsilon \approx 7.10^{-6}$ m^2 s^{-3} and by taking as a velocity scale the value obtained in the previous subsection for the standard deviation of the horizontal velocity, $\sigma_V \approx 2$ m s^{-1}:

$$T \approx \sigma_V^2/\varepsilon \approx 6.10^5 \text{ s} \approx 160 \text{ h}.$$

With a transport velocity of 5 m s^{-1}, this would mean a corresponding transport distance of about 3000 km for appreciable reduction of the kinetic energy, implying that transport can take place over many hundreds of kilometers without noticeable reduction of the kinetic energy.

The above is true for heights well above the boundary layer. From the turbulence measurements at 9 m, dissipation has been derived from inertial subrange spectra (cf. Smedman et al. 1997), the mean value for this period being 5×10^{-4} m^2 s^{-3}, which is about two orders of magnitude larger than the value found for the layers above. The height of the turbulent boundary layer is not more than a few tens of meters, thus comprising just a few percent of the 1000-m layer studied here.

c. Analysis of spectra of the horizontal components of the wind from the airborne measurements

The aircraft measurements of horizontal velocity from all but the last flight (which represented wind from over the island) and for all heights were evaluated as meridional and zonal components and were subjected to fast Fourier transform analysis to produce wavenumber spectra of the corresponding wind components.

Figure 9 shows the variation of spectral amplitude of the zonal component with height, plotted as the logarithm of $\kappa E(\kappa)$, for four selected wavenumbers, $\kappa = 10^{-3}$, 10^{-2}, 10^{-1}, and 1 radians m^{-1}. The plot gives computed mean values for the heights 30, 60, 90, 150, 210, 270, and 360 m as well as standard error of the mean, shown as horizontal bars. The figure reveals that the height variation, if any, is insignificant. An exactly

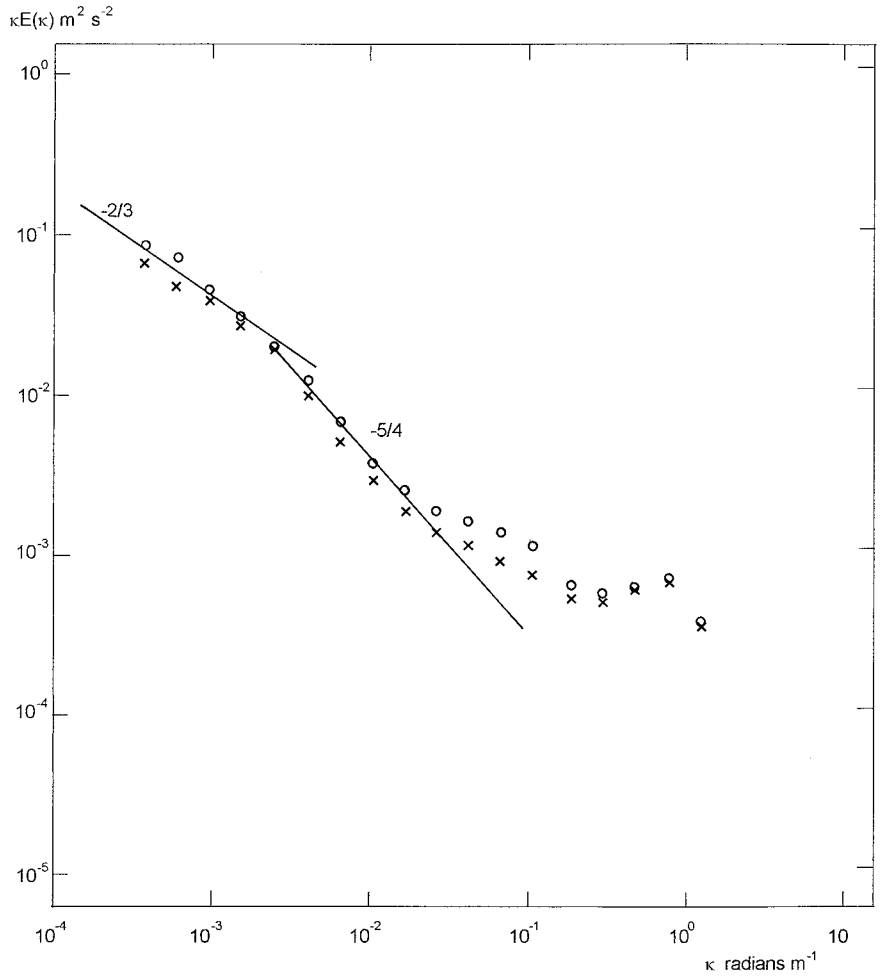

FIG. 10. Mean spectra of the zonal (rings) and meridional wind components (crosses), $\kappa E_{u,v}(\kappa)$ plotted on a log–log scale against wavenumber κ. Each symbol is an average over the first 10 flights and all the measuring heights (cf. Fig. 9) The straight lines have a slope of $-2/3$ and $-5/4$, respectively, corresponding to $E(\kappa) \sim \kappa^{-5/3}$ and $E(\kappa) \sim \kappa^{-9/4}$, respectively.

similar pattern is obtained for the meridional component (not shown here).

Figure 10 shows the overall (all flights, all heights) mean spectra for the zonal (rings) and meridional (crosses) components, plotted in a log–log representation of $\kappa E_{u,v}(\kappa)$ against κ. First it is noted that there are insignificant differences between the zonal and the meridional spectra. The data points in the spectral range $3 \times 10^{-4} \leq \kappa \leq 3 \times 10^{-3}$ radians m^{-1} scatter along a line with the slope $-2/3$, which corresponds to $E(\kappa) \sim \kappa^{-5/3}$. In the range $3 \times 10^{-3} \leq \kappa \leq 3 \times 10^{-2}$ radians m^{-1} the spectral slope is significantly larger; the line has been drawn corresponding to $E(\kappa) \sim \kappa^{-9/4}$. For higher wavenumbers the spectral slope again becomes appreciably smaller. Note that there is a gradual decrease of spectral energy with increasing wavenumbers, with no indication of a high wavenumber turbulent maximum and corresponding spectral gap.

The corresponding spectra measured at 9 m above the surface, presented in Smedman et al. (1997), show in most cases a turbulent maximum with a spectral level of about 10^{-2} m^2 s^{-2} at a frequency approximately corresponding to $\kappa \approx 0.3$ radians m^{-1} and sometimes a spectral minimum at $\kappa \approx 0.03$ radians m^{-1}. For lower frequencies these spectra rise steeply to levels similar to those of Fig. 10 at around $\kappa \approx 10^{-3}$ radians m^{-1}. In a few cases, turbulence was virtually nonexistent even at 9 m, with spectral curves monotonically decreasing with increasing frequency, as illustrated by Fig. 9 of Smedman et al.(1997). These spectra drop down to spectral levels as low as 3×10^{-5} m^2 s^{-2} at 10 Hz, with a value of about 10^{-4} at $n \approx \kappa = 1$ radians m^{-1}. This is about a factor of 5 lower than the corresponding spectral level of the aircraft data of Fig. 10. At $n \approx \kappa = 10^{-1}$ radians m^{-1} the spectral levels of the ''turbulence-free'' spectrum of Smedman et al. (1997) and that of our Fig. 10 are very close. It is probable that the aircraft spectral estimates at frequencies above about $\kappa = 10^{-1}$ radians

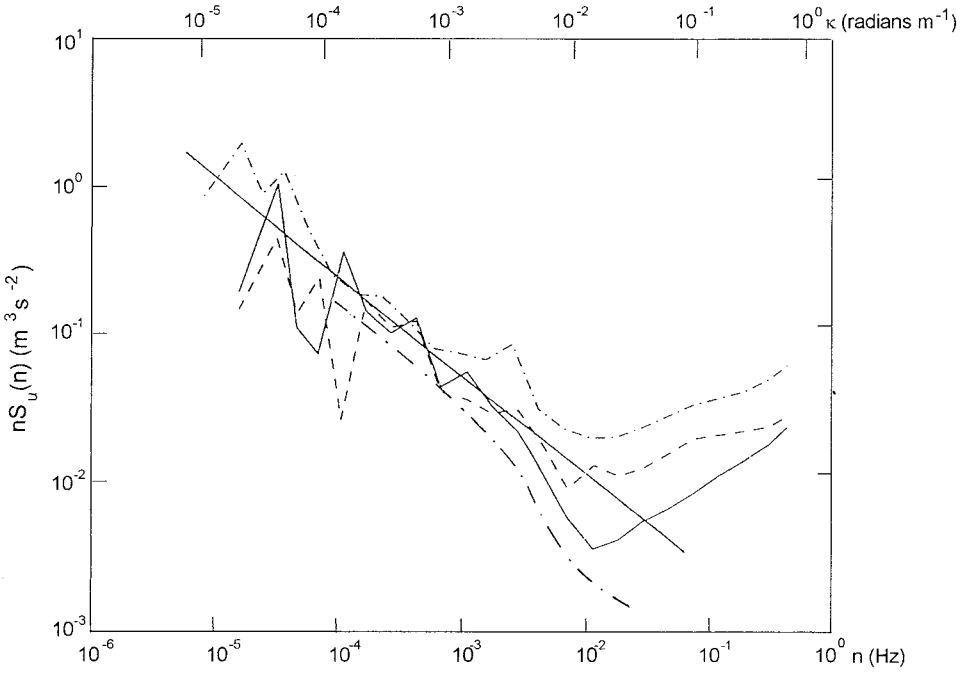

FIG. 11. Energy spectra of wind velocity between 8×10^{-6} and 0.5 Hz, derived from turbulence data (9 m) for three days. The line drawn corresponds to $-2/3$ slope of the $nSu(n)$-spectrum. The hatch-dotted line is the mean wavenumber spectrum taken from Fig. 10. The frequency scale has been transformed to a wavenumber scale by application of Taylor's transformation, taking the observed mean wind velocity of about 5 m s^{-1}.

m^{-1} is due to instrumental noise and that thus the apparent leveling off of the spectra in that range is an artifact. The 9-m spectra were obtained with the very sensitive MIUU instrument (Högström 1982, 1988) and are likely to give accurate spectral levels as low as those observed even at 10 Hz in the ''nonturbulent'' case. Thus it is to be expected that the spectrum of Fig. 10 in reality drops much faster with wavenumber above $\kappa \approx 10^{-1}$ radians m^{-1} than indicated by the plot.

The mean spectrum of Fig. 10 for the approximate frequency interval $10^{-4} \leq \kappa \leq 10^{-3}$ radians m^{-1} has been plotted along with the GASP spectra of Fig. 1. Our spectral levels are seen to be just a factor of about 2 lower than the GASP spectra, which were obtained from flights mainly in the upper troposphere and lower stratosphere.

d. Taylor-transformed frequency spectra from measurements on the tower

Energy spectra of the horizontal wind have been computed from three data segments of continuous measurements at the 9-m level on the tower, each of 48-h duration. In Fig. 11, $nS_u(n)$ has been plotted on a logarithmic scale against frequency n, also on a logarithmic scale. Here, ''u component'' refers to the component of the wind in the mean wind direction of each individual 48-h data segment. Over the frequency range 10^{-5} Hz $< n < 10^{-2}$ Hz the individual curves are seen to wriggle around a line with a $-2/3$ slope. Assuming Taylor's hypothesis to apply (cf. Brown and Robinson 1979) and taking the measured average wind of 5 m s^{-1}, this line, thus representing the average spectrum, can be compared with the mean wavenumber spectrum of Fig. 10, the hatch-dotted line. In the approximate wavenumber range $10^{-4} \leq \kappa \leq 3 \times 10^{-3}$ radians m^{-1} the mean aircraft spectrum and the mean Taylor-transformed frequency spectrum follow each other closely, the aircraft spectrum being about 50% lower throughout. The fact that the Taylor-transformed spectra rise systematically for wavenumbers above about 10^{-2} radians m^{-1} is entirely consistent with the presence of a turbulent part of the spectrum at the measuring height 9 m as discussed above.

e. Analysis of aircraft vertical velocity spectra

Figure 12 shows the height variation of $\log S_w(n)$ for the following frequencies: $n = 3 \times 10^{-4}$, 3×10^{-3}, 3×10^{-2}, and 3×10^{-1} Hz, respectively. It is clear that no systematic height variation is observed at the two lower frequencies. In contrast to this, there is a clear systematic decrease of the corresponding spectral amplitude in the lowest 100–200 m for the two highest frequencies.

Figure 13 shows the overall mean vertical velocity spectrum, derived from all the flights (except for the last one, as explained previously) and all heights. The

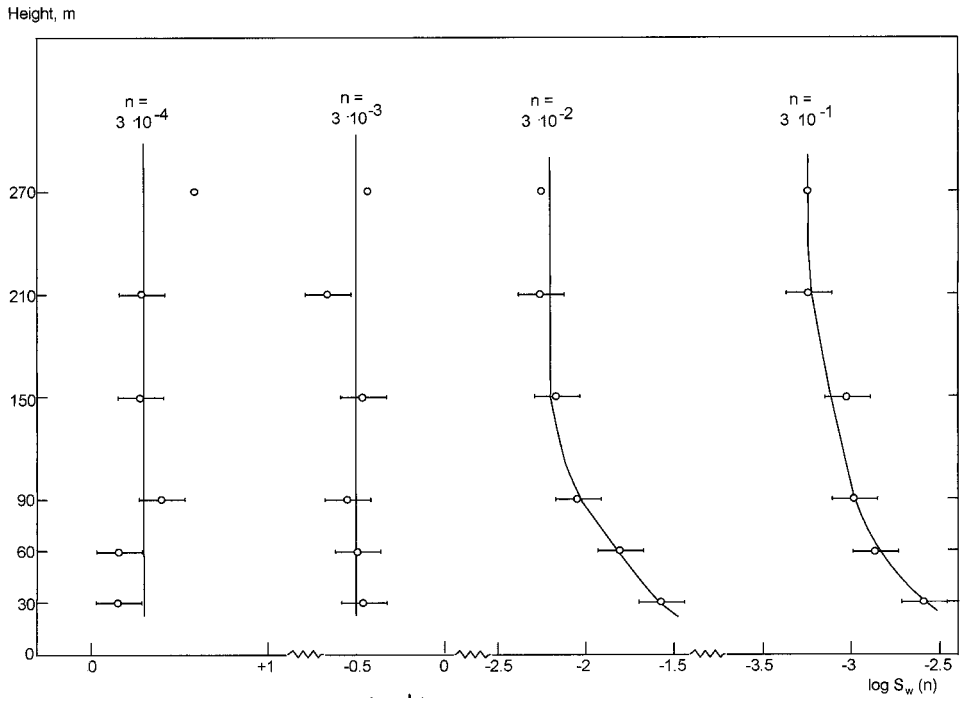

FIG. 12. The logarithm of the spectral amplitudes of the spectrum of vertical velocity, $S_w(n)$, for the 11 first flights, plotted as a function of measuring height for four selected frequencies, as indicated in the figure. The rings give mean values and the horizontal bars standard error of the mean.

plot gives $S_w(n)$ as function of frequency n in a log–log representation. Also included in the graph is the mean Doppler radar spectrum of Ecklund et al. (1986) as derived by them from several stations scattered around the world for ''low wind conditions'' or ''quiet-time conditions'' in the troposphere and in the stratosphere. Our mean spectrum agrees very well with their spectrum, except that our spectrum does not exhibit the ''bump'' near $n \approx 10^{-3}$ Hz. Ecklund et al. (1986) find that this feature is closely linked to the Brunt–Väisälä frequency. In our case the Brunt–Väisälä frequency is found at about an order of magnitude higher frequency, as indicated in Fig. 13. The agreement of our spectrum and the mean spectrum of Ecklund et al. (1986) applies in a remarkable degree not only to the shape of the spectrum (except for the bump area), with its ''flat'' shape at frequencies below about 8×10^{-4} Hz and the rate of rolloff at higher frequencies, but also to the spectral amplitude. In fact, integration of our mean spectrum gives the same vertical velocity variance, 10^{-2} m^2 s^{-2}, as that quoted by Ecklund et al. (1986).

Ecklund et al. (1986) make two general comments related to their quiet-time spectra: (i) they appear to have remarkable generality and (ii) they have close resemblance to spectra of internal waves in the ocean. The authors conclude that ''the quiet-time spectrum of vertical motions does seem to unambiguously represent a nearly universal spectrum of internal waves.'' The implication of this for interpretation of the present flow phenomenon will be discussed in section 6.

5. Analysis of the temperature field

a. Tower and sounding data

Looking at graphs of the daily course of temperature on the tower, like Fig. 6, it is found for each individual day that there is a pronounced maximum in late afternoon and early night. Also a minimum is found in the middle of the day. It is probable that these maxima and minima respectively reflect corresponding daytime temperature maxima and minima over the upstream land areas in the Baltic States with a lag of approximately 8 h, representing a transport distance of about 150 km and a mean wind speed of 5 m s^{-1}. An exact phase difference is not to be expected, because of random variations in transport distance and transport velocity.

If this interpretation of the large-scale temperature fluctuations in the tower recordings is correct, these fluctuations are likely to be present in a deep layer. Temperature autocorrelation plots derived from the radiosoundings, shown in Fig. 14, are very different from the wind autocorrelation plots of Fig. 8 in showing only little sign of vertical decorrelation, such decorrelation occurring primarily in the lowest 100-m layer. The general course of the temperature autocorrelation curves thus supports the idea that a large part of the temperature variance at each level is due to this advective effect. The total temperature standard deviation at 30 m is 3.1°C, at 100 m is 2.7°C, and at 200 m is 2.2°C, gradually decreasing to 1.3°C at 1000 m.

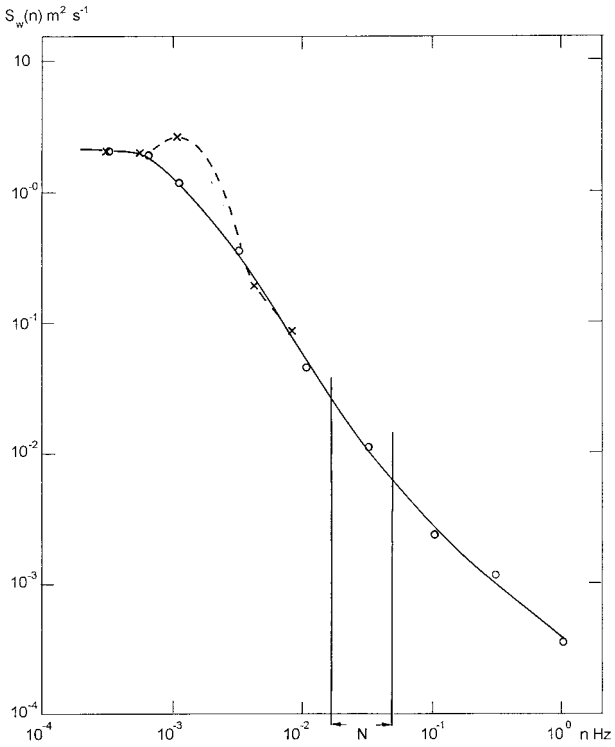

FIG. 13. Mean spectrum of vertical velocity, $S_w(n)$, plotted on a log–log scale against frequency n. The frequency range indicated by ''N'' is corresponding approximate range for the Brunt–Väisälä frequency encountered. Dashed line: average curve for quiet-time conditions of Ecklund et al. (1986).

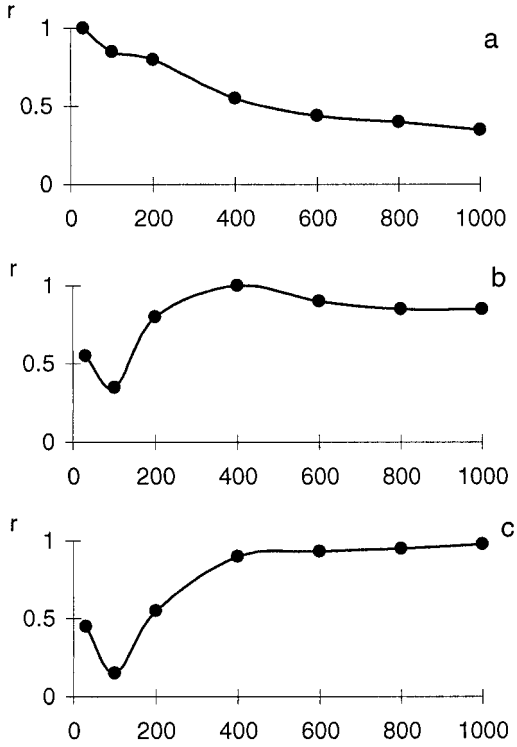

FIG. 14. Examples of autocorrelation plots for potential temperature similar to those for wind in Fig. 8. (a) How the correlation varies with height relative to the measurements at 30 m; (b) and (c) The correlation plotted relative to the measurements at 400 and 1000 m, respectively.

b. Analysis of airborne temperature spectra

In Fig. 15 are shown temperature spectra, $\kappa E_\theta(\kappa)$, against wavenumber κ in a log–log representation. Spectra from all flights (except the last one) have been taken together and divided into three height groups: 75, 152, and 248 m, respectively. The spectra exhibit a distinct variation with height, but their shape is quite similar for $\kappa < 10^{-1}$ radians m^{-1}. Also shown is the mean horizontal velocity spectrum taken from Fig. 10. It is seen to have exactly the same shape as the temperature spectra for $\kappa < 2 \times 10^{-2}$ radians m^{-1}.

Gage and Nastrom (1986a) find the same similarity of shape between their horizontal velocity spectra and their temperature spectra. They also find a systematic difference in spectral levels for their tropospheric and stratospheric temperature spectra, respectively. They show conclusively that this difference is due to the systematic difference in static stability of the troposphere and the stratosphere. They thus derive the following relation [their Eq. (6)] between the temperature spectrum $\Phi_{\theta\theta}$ (their notations are retained for simplicity) and the corresponding spectrum of potential energy Φ_{PE}:

$$\Phi_{\theta\theta} = \frac{2N^2\theta^2}{g^2}\Phi_{\text{PE}}. \tag{1}$$

When converting their temperature spectra into corresponding spectra of potential energy with the aid of this equation, Gage and Nastrom (1986a) find that their mean tropospheric and stratospheric spectra collapse. In our case static stability, and hence the Brunt–Väisälä frequency N, varies strongly and systematically with height. Thus, in the mean $N_{50\text{m}} \approx 4.6 \times 10^{-2}$ Hz and $N_{250\text{m}} \approx 2.2 \times 10^{-2}$ Hz. Assuming that Eq. (1) is valid also in our case and that, in addition, Φ_{PE} is constant, as found by Gage and Nastrom (1986), we would expect the ratio $(\Phi_{\theta\theta})_{50\text{m}}/(\Phi_{\theta\theta})_{250\text{m}}$ to be about 4.3. The corresponding spectral ratio has been evaluated from the measured spectra for the following wavenumbers: $\kappa = 3 \times 10^{-4}$, 10^{-3}, 3×10^{-3}, 10^{-2}, and 10^{-1} radians m^{-1}, giving the corresponding ratios 4.0, 5.1, 6.0, 4.9, and 4.9. The mean value is 5.0 ± 0.7 (standard deviation). This is not far from the ''theoretical value'' of 4.3, considering the uncertainty in the determination of the mean N values from the radio soundings. Taking only the two lowest wavenumbers, which are the ones that most closely fit into the range covered by the spectra of Gage and Nastrom (1986a), a mean value of 4.5 is obtained for the ratio, a value that is nearly identical to the theoretical value.

Gage and Nastrom (1986a) also consider the spectral ratio of kinetic to potential energy and find that it is close to 2, which is identical to the theoretical value

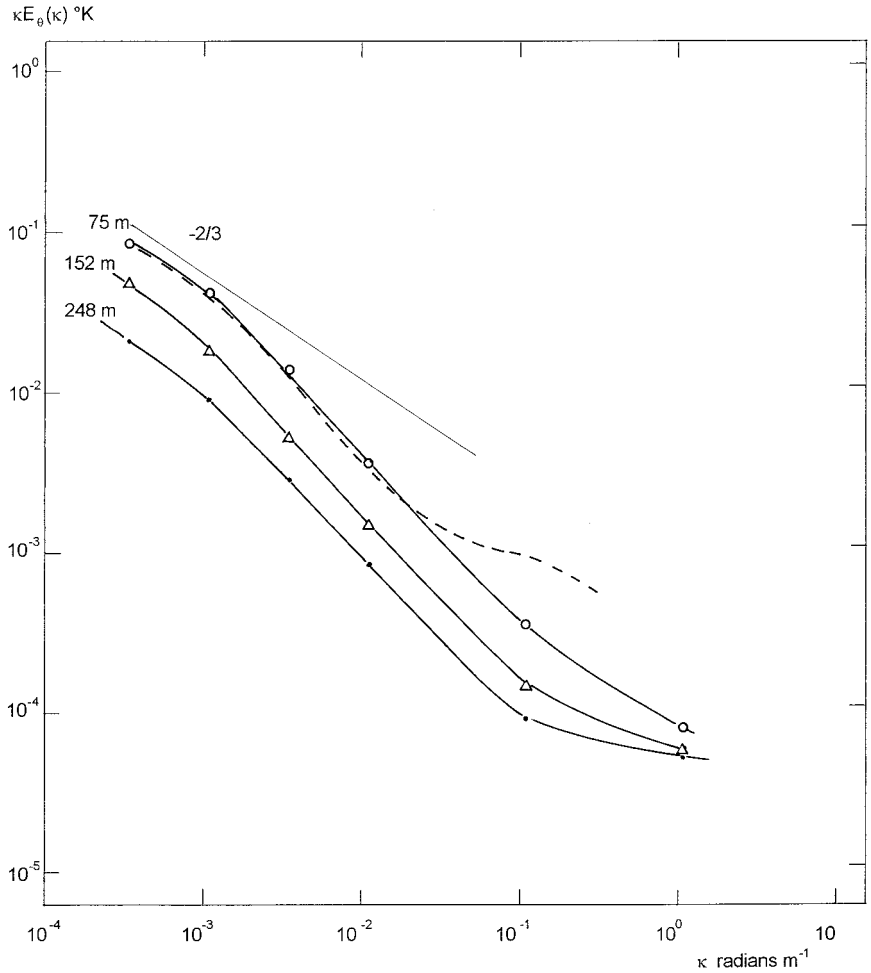

FIG. 15. Mean temperature spectra, $\kappa E_\theta(\kappa)$, as a function of wavenumber, κ, in a log–log representation. Data from all the 11 first flights and all the measuring heights have been divided into three height ranges, represented by the three curves labeled 75, 152, and 248 m, respectively. The hatched curve is the mean spectral curve for the zonal wind component taken from Fig. 10. The line with slope $-2/3$ corresponds to $E_\theta(\kappa) \sim \kappa^{-5/3}$.

deduced by Charney (1971) for geostrophic turbulence. Corresponding analysis of our spectra gives a value near 4 instead for the $-5/3$-range, that is, for wavenumbers below about 10^{-3} radians m^{-1}, and even higher ratios for higher wavenumbers.

6. Theoretical interpretation of the experimental results

In spite of several attempts, it has not yet been possible to make a definitive statement about the true nature and origin of the motions in the wavenumber range 10^{-5} $m^{-1} < \kappa < 10^{-3}$ m^{-1} from purely theoretical deductions. Kraichnan (1967) was probably the first to explore the characteristics of two-dimensional turbulence. From a similarity analysis he concluded that two kinds of inertial transfer regimes are possible: a regime where kinetic energy is conserved and cascaded along the spectrum in one particular direction and another range where squared vorticity (enstrophy) is conserved and transported along the spectrum in the opposite direction. He was not able from his formal analysis to conclude which are the actual cascade directions. He presented some evidence, however, to suggest that the energy cascade carries energy from smaller to larger scales and that the enstrophy cascade has the opposite direction, which is the same as that of the three-dimensional turbulence energy cascade. The following spectral expressions arose from Kraichnan's similarity analysis. For the upscale energy transfer:

$$E(\kappa) = C(dE/dt)^{2/3}\kappa^{-5/3}, \tag{2}$$

For the downscale enstrophy cascade:

$$E(\kappa) = C'\eta^{2/3}\kappa^{-3}, \tag{3}$$

where C and C' are constants, dE/dt is the net rate of energy transfer per unit mass, and η is the squared vorticity transfer.

Referring back to Fig. 1, it is seen that the observed GASP spectra follow Eq. (2) closely for the approximate wavenumber range 10^{-5} m^{-1} $< \kappa <$ 10^{-3} radians m^{-1} and Eq. (3) for a wavenumber range of slightly less than one decade below $\kappa = 10^{-5}$ radians m^{-1}. In terms of Kraichnan's (1967) theory, this could be interpreted as there being an enstrophy source near $\kappa = 10^{-6}$ radians m^{-1} and a kinetic energy source near $\kappa = 10^{-2}$ radians m^{-1}. Kraichnan makes, however, the following statement: ''The present paper has demonstrated some elementary consistency properties, but this does not show that the similarity ranges actually exist.''

Batchelor (1969) presented a similarity analysis related to the spectral development of two-dimensional turbulence after a sudden injection of turbulent energy, which resulted in the following form:

$$E(\kappa) = 1/2V'^3 tg(V'\kappa t), \tag{4}$$

where V' is the standard deviation of the turbulent fluctuations, t is time after injection, and g is an undetermined function of $V'\kappa t$. According to this relation, the energy of the turbulence is simply moving into larger length scales, just as suggested by Kraichnan (1967).

Lilly (1983) carried out a scale analysis of several kinds of motions that may result from release of originally three-dimensional turbulent kinetic energy into a stratified environment. He found that both waves and stratified two-dimensional turbulence could result from such a release and that in fact they are likely to occur in about equal proportions. He further argued that the wave energy is likely to propagate to the stratosphere in minutes to hours and then to suffer turbulent breakdown.

VanZandt (1982) has, however, suggested that wave energy could be reflected back and in fact create irregular wavelike motions giving rise to a spectrum of the form described by Eq. (2). As pointed out by Gage and Nastrom (1986a), the wave theory includes, however, elements of internal consistency requirements that can be tested against measurements. Such a test was carried out by these authors, and they came to the conclusion that the GASP spectra cannot possibly be caused by gravity waves. Instead they suggested that their horizontal velocity spectra for the range $10^{-5} < \kappa < 10^{-3}$ radians m^{-1} must be the manifestation of two-dimensional stratified turbulence. But they also came to the conclusion that ''the vertical velocity spectra reflect internal wave activity.'' In order to come to a conclusion about the physical nature of the flow phenomenon found in the present study, the data will be subjected to a similar treatment as that of Gage and Nastrom (1986a).

It is first worth noticing that the present data extend to much higher wavenumbers than the GASP spectra. In fact, the present data contain the spectral region around $\kappa \approx 10^{-2}$ radians m^{-1}, which Gage and Nastrom (1986a) designate a possible source region for the upscale energy transfer. If this is so, we would expect the approximate spectral region 10^{-3} m^{-1} $< \kappa < 10^{-1}$ radians m^{-1} to contain breaking waves or possibly a mixture of breaking waves and two-dimensional stratified turbulence. In this respect it is a notable feature of the horizontal velocity spectra in Fig. 10 that the spectral slope in this region is much larger than in the region $\kappa < 10^{-3}$ radians m^{-1}. In fact, as noted earlier, $E(\kappa) \sim \kappa^{-9/4}$, which is close to the VanZandt (1982) prediction from wave theory that $E(\kappa) \sim \kappa^{-2.5}$ for this spectral region.

Gage and Nastrom (1986b) make use of the polarization relation for internal waves to test if their spectra could possibly be a manifestation of such waves:

$$\frac{2\Phi_{uu}}{\Phi_{ww}} = \frac{N^2 - \omega^2}{\omega^2}. \tag{5}$$

Here N is, as before, the Brunt–Väisälä frequency and ω is circular frequency $2\pi n$. With the present data at hand this relation can be checked directly for every desired frequency, provided the Taylor transformation $\kappa = \omega/U$ is made and there is no need to do the rather indirect calculation of Gage and Nastrom (1986b). For wavenumbers below and up to about 10^{-3} radians m^{-1}, the ratio $\omega_p/\omega_o \approx 3$, with ω_p = the frequency derived from Eq. (5) and ω_o = the frequency value obtained from the Taylor transformation, which thus negates the hypothesis that the flow presented by this spectral region is governed by internal waves. For $\kappa = 10^{-2}$ radians m^{-1}, the corresponding ratio is close to 1. Thus, the polarization relation, Eq. (5) is not valid for $\kappa < 10^{-3}$, that is, the region of $E(\kappa) \sim \kappa^{-5/3}$, but is approximately valid in the range around $\kappa = 10^{-2}$ radians m^{-1}.

Another test of the nature of the flow in the spectral range of wavenumbers below about 10^{-3} radians m^{-1} is provided by the prediction from wave theory quoted by Gage and Nastrom (1986a) that ''velocity spectral amplitudes will increase with N.'' As mentioned in the previous section, N decreases systematically with height in the present data, the ratio $N_{50\text{m}}/N_{250\text{m}}$ being about 2. But, as clearly demonstrated in Fig. 9, no corresponding height variation of the amplitudes of the horizontal velocity spectra is observed. It is also notable that the present spectra are a factor of 2 lower than the GASP spectra, which represent N values 2–4 times smaller than the present data.

The analysis of vertical velocity autocorrelation presented in section 4a and shown graphically in Fig. 8 gives another strong argument for the idea that the horizontal motions in the spectral range below $\kappa \approx 10^{-3}$ radians m^{-1} are due to two-dimensional stratified turbulence and not internal waves. As shown in section 4a, the measured autocorrelation half-width is of the order a few hundred meters. This contrasts sharply to the predictions from wave theory by VanZandt (1982), who finds the correlation half-width to be 7.7 km, but it is in complete agreement with Lilly's (1983) prediction that flow in two-dimensional stratified turbulence is expected to occur in vertically decorrelated layers.

Lilly (1983) had some concern about possible breakdown of the flow with such strong shear being produced by this layering of the flow. As shown in section 4b, the present situation did not, however, lead to rapid turbulent dissipation. On the contrary, the rate of dissipation is found to be so low that the flow is likely to persist over transport distances of the order at least several hundreds of kilometers.

Gage and Nastrom (1986a) compare their GASP wavenumber spectra with other spectra derived from Taylor transformation of frequency spectra and find very good agreement. They conclude that ''the success of the Taylor transform is a strong indication that the GASP spectra represent a nondispersive turbulence-like process.'' It is notable that the same good agreement is found in the present study between aircraft-derived wavenumber spectra and Taylor-transformed frequency spectra from the tower, as discussed in section 4d.

As discussed in section 4e, the agreement between the mean vertical velocity spectrum of the present study and the average universal quiet-time spectrum of Ecklund et al. (1986) is remarkable in many respects. Gage and Nastrom (1986b) conclude that ''the atmospheric spectrum of vertical velocity closely resembles an internal wave spectrum with a basically flat shape and a sharp cutoff near the Brunt–Väisälä frequency.'' In the latter respect the present spectra (Fig. 13) show a peculiar deviation from the corresponding Ecklund et al. (1986) spectra in having a Brunt–Väisälä frequency an order of magnitude larger and not having the associated bump that is so characteristic of the spectra of these authors. It is hard to see any obvious explanation for this feature. It looks like the wave activity is being governed by processes much higher up in the troposphere, but this is just speculation.

The role of internal waves in relation to the present flow situation is intriguing. Gage and Nastrom (1986a) consider the horizontal and vertical motions as the result of separate atmospheric processes, the flow being basically quasi-horizontal but modified by sliding over waves, which produces the vertical velocity fluctuations. This is very probably the situation in the present case as well.

The true nature of the flow in the spectral region around $\kappa = 10^{-2}$ radians m^{-1} is more difficult to settle. It has been noted above that the region has some characteristics relevant to internal waves, that is, the spectral falloff of the horizontal velocity spectra of Fig. 10 is not far from the predicted $E(\kappa) \sim \kappa^{-2.5}$, and also that the polarization relation, Eq. (5), is approximately valid.

Another potential indicator of wave activity are co- and quadrature spectra of vertical velocity and temperature. Such spectra have been evaluated for each flight and measuring height. Analysis of these spectra gives, however, very little information that can be used for interpretation of the flow regime. For $\kappa > 10^{-2}$ radians m^{-1}, both the co- and quadrature spectra have virtually zero spectral energy. For lower frequencies both types of spectra exhibit random variations. For $\kappa Co_{w\theta}(\kappa)$ and $\kappa Q_{w\theta}(\kappa)$ these random peaks typically reach a magnitude of $\pm 10^{-2}$ m s^{-1} K in spectra of individual flight legs. Mean spectra for any flight or for any particular height have typically spectral amplitudes an order of magnitude or more less than this and with standard deviation several times bigger than the corresponding mean values. This result is perhaps not surprising, considering the expectation that the spectral region around $\kappa \approx 10^{-2}$ radians m^{-1} is likely to be the source region for the larger-scale quasi-two-dimensional stratified turbulence. It is thus likely to contain breaking waves, implying that the criterion discussed by Finnigan (1988) that the cross spectrum of the vertical velocity and temperature wave components exhibit a large quadrature spectrum in association with small cospectrum is certainly not valid, as it is only true for precisely linear behavior of the wave.

7. Conclusions

The analysis of the data has clearly demonstrated that for wavenumbers smaller than about 10^{-3} radians m^{-1} the flow studied here bears close similarity to the flow regime in the approximate wavenumber range $10^{-5} \leq \kappa \leq 10^{-3}$ radians m^{-1} of the GASP spectra studied by Nastrom and Gage (1985) and Gage and Nastrom (1986a,b). Thus the spectra of the horizontal components are proportional to $\kappa^{-5/3}$ in both studies and with spectral amplitudes just a factor of 2 less for the present study. Temperature spectra were found to parallel the horizontal velocity spectra like it did in the GASP study (Gage and Nastrom 1986b). Also, the scaling of the spectral amplitudes of the temperature spectra with the local Brunt–Väisälä frequency was found to apply here.

Vertical velocity spectra were not obtained directly from the GASP project. Gage and Nastrom (1986a) instead used available data from ground-based Doppler radar measurements from a few places scattered over the globe. They noticed strong universality of spectra measured during ''quiet-time conditions.'' The aircraft spectra from the present study are very similar to those ''universal'' spectra, not only in shape but also in spectral amplitude and total variance, the only remarkable difference being that the change in spectral shape from flat to rapid drop does not occur at the local Brunt–Väisälä frequency as observed in the Doppler radar spectra, but at a much lower frequency. Nevertheless, the conclusion of Gage and Nastrom (1986a) that the Doppler spectra are likely to reflect internal wave spectra appears equally valid in the present case.

Gage and Nastrom (1986a) tested several criteria that must be fulfilled for the observed horizontal velocity spectra to be a manifestation of internal gravity waves, as suggested by VanZandt (1982), and they found that this could not possibly be the case for the horizontal motion. Similar analysis done here gives essentially the

same result, strong additional evidence being given by the observation that vertical decorrelation of the flow takes place over a height interval of a few hundred meters only, in sharp contrast to the 7.7 km predicted for the wave case by VanZandt (1982). It is notable that this kind of rapid vertical decorrelation of the quasi-horizontal flow was predicted to occur in two-dimensional stratified turbulence by Lilly (1983).

To conclude the discussion of the flow representing wavenumbers below about 10^{-3} radians m^{-1}, the analysis substantiates the conclusion reached by Gage and Nastrom (1986a) that the horizontal and vertical velocity spectra are characteristic of separate atmospheric processes; that is, the horizontal velocity spectra reflect quasi two-dimensional turbulence but the vertical velocity spectra wave activity.

For the wavenumber decade above about 10^{-3} radians m^{-1} the situation is much less clear. According to, for example, Gage and Nastrom (1986a) the likely source of energy for the upscale cascade process leading to the flow regime discussed above, is expected to be found here, probably in the form of breaking internal waves. The spectral slope for the horizontal velocity spectra in this range, $E(\kappa) \sim \kappa^{-2.3}$, is close to that predicted from wave theory by VanZandt (1982), who gets an exponent of -2.5. Also, the polarization relation seems to be approximately valid. No signature of wave activity is found in the temperature–vertical velocity cross spectra, but that would hardly be expected for breaking gravity waves. In conclusion, there is certainly some evidence in the present data to support the idea that the spectral range near $\kappa \approx 10^{-2}$ radians m^{-1} is indeed the site of internal waves that may be breaking and producing the energy needed for the upscale cascade of energy.

Acknowledgments. The authors would like to thank the staff from the Department of Meteorology, Uppsala (now the Department of Earth Sciences, Meteorology), who made the field experiments possible. This includes Mr. Knut Lundin, who is responsible for electronic design and construction of the instrumentation on the tower, Ms. Birgitta Källstrand, Ms. Anna Rutgersson, Dr. Mikael Magnusson, and Mr. Stefan Sandström, who carried out all radiosoundings and pilot balloon measurements, and Mr. Patrick Samuelsson and Dr. Michael Tjernström, who were responsible for the airborne measurements. The costs for establishing the Östergarnsholm field station was defrayed by grants from the Natural Science Research Council (NFR) Contract G-AA/GU 03556-313 and from the Swedish National Energy Administration, Grant 506 226-4. The airborne measurements were financed from a grant from the EU-JOULE programme, JOU2-CT93-0325. The work of the second author was made possible by a grant from NFR, Contract S-AA/FO 03556-314.

APPENDIX

The Cause of the Unexpectedly Deep Stable Layer Observed near the Surface at Östergarnsholm

With the large temperature contrast between the daytime land surfaces of the upwind area of the Baltic States (and, sometimes, Poland) on one hand and that of the sea surface on the other hand, a much more shallow stable layer would have been expected. Simulations of the present situation with the MIUU numerical boundary layer model gives the answer. The model (Enger 1990) has a level 2.5 turbulence parameterization, and its ability to simulate situations similar to the present have been proven in several previous studies, for example, Bergström (1996). For simulation of the present case, the model was run both in a two-dimensional mode and in a three-dimensional mode.

The 2D version was run along a transect in the mean wind direction from the Baltic States, through Östergarnsholm, and farther across the island of Gotland, with a resolution of 1 km in the central area of interest and telescopingly increasing grid size toward the outer parts of the model domain. The model was run for one particular day, and input to the model were estimated roughness of upwind land areas and of the sea surface and the island of Gotland, respectively; estimated daily course of surface temperature of the upwind areas in the Baltic States and Gotland and a constant sea surface temperature; and geostrophic wind speed and direction. The model was initiated with data from a radiosounding, representing the conditions at 0000 UTC.

The model was run both for the actual case and for several cases where some of the conditions were changed, such as the roughness and the temperature of Gotland. The result is quite clear: taking away the downwind roughness change represented by Gotland gives at Östergarnsholm the very shallow stable boundary layer expected. In sharp contrast, the actual situation produces a stable layer at Östergarnsholm that is much deeper and very well matches the measured profile shown in Fig. 4. Keeping the surface temperature of Gotland constant and equal to that used for the sea surface does not change this situation much. Thus the conclusion is that it is the downwind roughness change offered by the big island of Gotland that is causing a blocking effect, which, in turn, produces the observed temperature profiles.

Runs were also done with a 3D version of the model, with a resolution of 2 km in the central simulation domain. These simulations contain a lot of details, which are due to the complex coastal topography of the Gotland coastline, but the blocking effect is simulated in a similar way as with the 2D version of the model.

REFERENCES

Batchelor, G. K., 1969: Computation of the energy spectrum in homogeneous two-dimensional turbulence. *Phys. Fluids (Suppl. II),* 233–239.

Bergström, H., 1996: A climatological study of boundary layer wind speed using a meso-γ-scale higher order closure model. *J. Appl. Meteor.,* **35,** 1291–1306.

Brown, E. N. C., C. H. Friehe, and D. H. Lenschow, 1983: The use of pressure fluctuations on the nose of an aircraft for measuring air motion. *J. Climate Appl. Meteor.,* **22,** 171–180.

Brown, P. S., and G. D. Robinson, 1979: The variance spectrum of tropospheric winds over eastern Europe. *J. Atmos. Sci.,* **36,** 270–286.

Charney, J. G., 1971: Geostrophic turbulence. *J. Atmos. Sci.,* **28,** 1087–1095.

Ecklund, W. L., K. S. Gage, G. D. Nastrom, and B. B. Balsey, 1986: A preliminary climatology of the spectrum of vertical velocity observed by clear-air Doppler radar. *J. Climate Appl. Meteor.,* **25,** 885–892.

Enger, L., 1990: Simulation of dispersion in moderately complex terrain. Part A. The flow dynamic model. *Atmos. Environ.,* **24A,** 2431–2446.

Finnigan, J. J., 1988: Kinetic energy transfer between internal gravity waves and turbulence. *J. Atmos. Sci.,* **45,** 486–505.

Gage, K. S., and G. D. Nastrom, 1986a: Theoretical interpretation of atmospheric wavenumber spectra of wind and temperature observed by commercial aircraft during GASP. *J. Atmos. Sci.,* **43,** 729–740.

——, and ——, 1986b: Spectrum of atmospheric vertical displacements and spectrum of conservative scalar passive additives due to quasi-horizontal atmospheric motions. *J. Geophys. Res.,* **91,** 13 211–13 216.

Högström, U., 1982: A critical evaluation of the aerodynamical error of a turbulence instrument. *J. Appl. Meteor.,* **21,** 1838–1844.

——, 1988: Non-dimensional wind and temperature profiles in the atmospheric surface layer: A re-evaluation. *Bound.-Layer Meteor.,* **42,** 55–78.

Kraichnan, R. H., 1967: Inertial ranges in two-dimensional turbulence. *Phys. Fluids,* **10,** 1417–1423.

Larsen, M. F., M. C. Kellet, and K. S. Gage, 1982: Turbulence spectra in the upper troposphere and lower stratosphere between 2 hours and 40 days. *J. Atmos. Sci.,* **39,** 1035–1041.

Lilly, D. K., 1983: Stratified turbulence and the mesoscale variability of the atmosphere. *J. Atmos. Sci.,* **40,** 749–761.

Nastrom, G. D., and K. S. Gage, 1985: A climatology of atmospheric wavenumber spectra of wind and temperature observed by commercial aircraft. *J. Atmos. Sci.,* **42,** 950–960.

Smedman, A., U. Högström, and H. Bergström, 1997: The turbulence regime of a very stable marine air flow with quasi-frictional decoupling. *J. Geophys. Res.,* **102,** 21 049–21 059.

Tjernström, M., and C. A. Friehe, 1991: Analysis of radome air-motion system on a twin-jet aircraft for boundary-layer research. *J. Atmos. Oceanic Technol.,* **8,** 19–40.

VanZandt, T. E., 1982: A universal spectrum of buoyancy waves in the atmosphere. *Geophys. Res. Lett.,* **9,** 575–578.